Cellular/Molecular

Initiation and Propagation of Action Potentials in Gonadotropin-Releasing Hormone Neuron Dendrites

Karl J. Iremonger and Allan E. Herbison

Centre for Neuroendocrinology, Department of Physiology, University of Otago School of Medical Sciences, Dunedin 9054, New Zealand

Gonadotropin-releasing hormone (GnRH) neurons are the final output neurons in a complex neuronal network that regulates fertility. The morphology of GnRH neuron dendrites is very different to other central neurons in that they are very long, thin, and unbranched. To study the function of these dendrites, we have used Na^+ and Ca^{2+} imaging in combination with dual soma and dendrite electrical recordings in brain slices from GnRH-GFP mice. Here, we show that GnRH neurons actively propagate Na^+ spikes throughout their dendrites. Multisite dendritic recordings confirmed that these spikes were observed in one of the dendrites before the soma in the great majority of neurons tested. Na^+ imaging experiments revealed that the initial 150 μm of dendrite has a higher density of functional Na^+ channels than more distal regions, suggesting that this region of dendrite is highly excitable and may be the site of spike initiation. Finally, we show that the depolarization from dendritic spikes opens voltage-gated Ca^{2+} channels giving rise to dendritic Ca^{2+} transients. Together, these findings suggest that the proximal dendrites of GnRH neurons are highly excitable and are likely to be the site of action potential initiation in these neurons.

Introduction

Gonadotropin-releasing hormone (GnRH) neurons are the final output cells of the neural network regulating fertility. They synthesize GnRH peptide that is released from their nerve terminals in the median eminence to regulate luteinizing and follicle-stimulating hormone release from the anterior pituitary and thus reproductive function (Moenter et al., 2003; Herbison, 2006). In adult mice, GnRH neurons are most commonly unipolar or bipolar with very long, unbranched dendritic processes (Campbell et al., 2005; Ybarra et al., 2011). While the long thin processes emanating from the cell body of most GnRH neurons possess spines and have a dendritic morphology (Jennes et al., 1985; Wray and Hoffman, 1986; Campbell et al., 2005, 2009; Cottrell et al., 2006), the origin of the GnRH neuron axon remains undetermined. Recent evidence, however, has suggested that the dendrite may be the site of action potential initiation in these neurons (Roberts et al., 2008).

While many neurons are capable of conducting action potentials throughout their dendrites (Stuart and Sakmann, 1994; Häusser et al., 1995; Golding and Spruston, 1998), very few initiate spikes in their dendrite (Chen et al., 1997; Martina et al., 2000). In the vast majority of neurons studied, the action potential is first initiated in the axon initial segment, as this region of the neuron has both a hyperpolarized shift in the activation voltage of Na^+ channels and the highest density of voltage-gated Na^+ channels (Colbert and Pan, 2002; Kole et al., 2008; Hu et al., 2009; Fleidervish et al., 2010). Interestingly, dual recordings from the soma and dendrite of GnRH neurons suggest that some GnRH neurons may initiate action potentials first in their dendrite (Roberts et al., 2008). It is currently unclear how common this dendritic initiation of spiking is. Moreover, it is unknown whether one region of the GnRH neuron dendrite is more excitable than others. Finally, the ionic nature of these dendritic spikes and how far they propagate through the dendritic arbor is yet to be determined. Here, we address these questions using combined electrophysiology with laser-scanning confocal microscopy in brain slices.

Received July 21, 2011; revised Oct. 7, 2011; accepted Nov. 7, 2011.

Author contributions: K.J.I. and A.E.H. designed research; K.J.I. performed research; K.J.I. analyzed data; K.J.I. and A.E.H. wrote the paper.

This work was supported by grants from the Health Research Council of New Zealand. We thank Dr. Colin Brown, Dr. Xinhuai Liu, Dr. Richard Piet, and Michel Herde for helpful comments on this manuscript.

Correspondence should be addressed to Prof. Allan E. Herbison, Centre for Neuroendocrinology, Department of Physiology, University of Otago School of Medical Sciences, P.O. Box 913, Dunedin 9054, New Zealand. E-mail: allan.herbison@otago.ac.nz.

DOI:10.1523/JNEUROSCI.3739-11.2012

 0270-6474/12/320151-08$15.00/0

Materials and Methods

Slice preparation

All experiments were approved by the University of Otago Animal Welfare and Ethics Committee. Male C57BL/6J GnRH-GFP mice (Spergel et al., 1999) (1–6 months of age) were killed by cervical dislocation, after which their brain was quickly removed and placed in ice-cold oxygenated (95% O_2/5% CO_2) cutting solution, which consisted of the following (in mM): 87 NaCl, 2.5 KCl, 25 $NaHCO_3$, 1.25 NaH_2PO_4, 0.5 $CaCl_2$, 6 $MgCl_2$, 25 D-glucose, 75 sucrose. Sagittal brain slices, 250 μm thick, containing the medial septum and rostral preoptic area, were then cut on a vibratome (Leica; VT1000S) and subsequently kept in oxygenated artificial cerebrospinal fluid (ACSF) at 32°C. ACSF consisted of the following (in mM): 118 NaCl, 3 KCl, 11 D-glucose, 10 HEPES, 25 $NaHCO_3$, 2.5 $CaCl_2$, 1.2 $MgCl_2$. Slices were incubated for a minimum of 60 min before patch-clamp recordings.

Electrophysiology

Slices were placed in a recording chamber under an Olympus BX61WI microscope and continuously superfused with oxygenated ACSF (95% O_2/5% CO_2) at a rate of 1–2 ml/min. Recordings were performed at 25°C. In this current study, we targeted GnRH neurons with a simple morphology (one or two primary processes) primarily located in the rostral pre-

optic area and medial septum. Previous work has shown that these processes have a dendritic morphology and possess dendritic spines (Campbell et al., 2005, 2009). Based on this and on the morphology of these processes we visualized in the living brain slices, we have also defined these processes as dendrites. Axonal processes positive for GFP could be visualized in brain sections containing the median eminence. Axons were very thin and had a beaded appearance. These look very different to the dendritic processes we imaged and recorded from.

Whole-cell recordings. The pipette solution for whole-cell recording consisted of the following (in mM): 140 potassium gluconate, 8 NaCl, 10 HEPES, 10 tris-phosphocreatine, 4 MgATP, 0.4 NaGTP, pH 7.2 with KOH. For whole-cell voltage-clamp experiments, neurons were clamped at −60 mV. The pipette junction potential was calculated to be −15.4 mV and was not subtracted.

On-cell recordings. Loose seal on-cell recordings were performed with pipettes filled with ACSF. Somatic and dendritic recordings were performed in voltage clamp with the holding current kept at 0 pA. For dendritic on-cell recordings, the dendrite was traced by confocal imaging of the GFP signal. Light suction was applied to the dendrite and a dendritic loose seal was assumed to have formed if there was a simultaneous increase in the pipette resistance as well as the existence of a small amount of GFP-labeled membrane in the tip of the pipette.

Extracellular recordings. Patch pipettes were filled with 150 mM NaCl and placed near different parts of the recorded cell to record extracellular field potentials (Palmer et al., 2010). Whole-cell recordings were simultaneously performed from the soma in current clamp. Alexa Fluor 555 hydrazide (40 μM) was included in the whole-cell pipette solution to visualize cell morphology. Small amounts of constant current were injected into the cell to induce action potential firing. Action potentials were detected with on-line spike triggered averaging (normally 100–200 sweeps).

Glutamate puffing. For glutamate/glycine puff experiments, patch pipettes (7–10 MΩ) were filled with ACSF, 1 mM glutamate, and 1 mM glycine. The tip of the puff pipette was positioned below the surface of the slice and a 2 s, low-pressure (~0.4 psi) puff was delivered with an attached syringe. No depolarization was seen at the soma when the puff pipette was moved ~70 μm away from the soma/dendrite. Picrotoxin (100 μM) was included in the bath ACSF for these experiments.

Confocal imaging

Imaging was performed with an Olympus FV1000 confocal microscope fitted with a 40×, 0.8 NA objective lens. eGFP and CoroNa Green were excited with a 488 nm argon laser (Melles Griot). Emitted light was detected by a photomultiplier tube (PMT) after passing through a bandpass filter (505–605 nm). Rhod-2 was excited with a 543 nm HeNe laser (Melles Griot) and fluorescence was detected by a PMT after passing through a 560–660 nm bandpass filter. The confocal aperture was wide open during Ca^{2+} and Na^{+} imaging experiments so as to collect the most emitted fluorescence.

Neurons were loaded with dyes via the patch pipette for a minimum of 15–20 min before imaging experiments were performed. Ca^{2+} imaging was performed with 500 Hz line scans oriented parallel along the dendrite of interest. For Na^{+} imaging experiments, we chose to use CoroNa Green instead of sodium-binding benzofuran isophthalate (SBFI) because we lack a suitable UV laser line for SBFI excitation. Both of these Na^{+} indicator dyes emit in the green spectrum, which may be problematic when loading GFP neurons. Because of this, in the majority of our analysis we did not normalize to the baseline fluorescence. In addition, the sensitivity of CoroNa is less than other Na^{+} indicators (Meier et al., 2006); therefore, to increase the signal-to-noise ratio, we performed frame scans at 15 Hz and averaged the responses across 5–10 trials. Changes in fluorescence were calculated for somatic or dendritic regions of interest.

Data collection and analysis

Electrophysiological recordings were collected with a Multiclamp 700B amplifier (Molecular Devices), using a low-pass filter at 1 kHz and digitized with the Digidata 1440A (Molecular Devices) at 50–100 kHz. For dual whole-cell and extracellular recordings, signals were filtered at 6 kHz and digitized at 100 kHz.

All electrophysiological data were analyzed with Clampex 10 software (Molecular Devices). For dual on-cell recordings, latency between somatic and dendritic spikes was determined by averaging the time between the peak of the somatic and dendritic spike. For dual whole-cell and extracellular recordings, analysis was performed on the spike-triggered average traces. Latency was determined between the peak of the first derivative of the somatic spike recorded in whole-cell mode and the peak of the extracellular spike. The latency of the extracellularly recorded spike at the soma was defined as 0 ms and all latency comparisons were made relative to this.

Imaging data were analyzed with Fluoview 1000 software (Olympus) and ImageJ. Fluorescence transients are expressed as either $\Delta F/F$ or ΔF. $\Delta F/F = (F - F_0)/F_0$, where F is the fluorescence and F_0 is the baseline fluorescence. F was calculated after subtracting background fluorescence. For Ca^{2+} imaging, the peak Ca^{2+} transient was obtained by averaging a period of 100 ms around the peak. The peak Na^{+} fluorescence transient was calculated from the average fluorescence in the dendritic region of interest of the last five frames during the 10 Hz spike train. The diameter of the dendrite at the imaging site was measured from single image planes.

All data are presented as mean ± SEM. Statistical analyses were performed with either paired t tests or repeated-measures ANOVA with a *post hoc* Newman–Keuls test. A value of $p < 0.05$ was accepted as statistically significant.

Results

Na^{+} spikes are observed first the dendrites of some GnRH neurons

To examine the location of spontaneous spike initiation in GnRH neurons, we performed dual on-cell (loose seal) recordings from the soma and dendrite (Fig. 1). The distance from the soma at which dendritic recordings were performed ranged from 68 to 417 μm (mean distance, 203.5 ± 13.3 μm; $n = 39$). Once dual recording was established, neurons were allowed to fire spikes spontaneously. In 30.8% of recorded cells (12 of 39), spontaneous spikes were first detected at the dendritic recording electrode before the somatic electrode (mean latency difference, −0.20 ± 0.06 ms; mean distance, 185.4 ± 14.3 μm; $n = 12$). In the remaining 27 neurons, spikes were recorded first at the somatic electrode before the dendritic electrode (mean latency between spikes, 0.20 ± 0.03 ms; mean distance, 211.6 ± 18.2 μm; $n = 27$). Failure of spike propagation between the two recording sites was never observed. These data show that some GnRH neurons are capable of spontaneously initiating spikes in regions beyond the soma.

Relative timing of spikes at multiple sites along GnRH neuron dendrites

The number of GnRH neurons that showed spikes in the dendrite before the soma was only 30% based on on-cell recordings from the soma and one dendritic site. To determine whether this low percentage was simply because we only recorded from one dendritic site on only one dendrite, we performed multisite recordings. It has previously been shown that multisite on-cell recordings can introduce significant errors in the estimation of the spike latency because of a temporal overlap of action potential evoked ionic and capacitive currents. However, these errors can be mitigated by recording the local extracellular action potential (eAP) (Palmer et al., 2010).

Whole-cell recordings were performed from the soma of GnRH neurons. A small amount of constant current was injected into cells to induce tonic action potential firing. A second extracellular field potential electrode was placed at multiple sites along the soma-dendritic axis of the recorded GnRH neuron. Because the amplitude of the eAPs was very small, we could only record extracellular spikes in proximal regions of the dendrite (generally <100 μm from the soma). Dendritic eAPs that occurred before

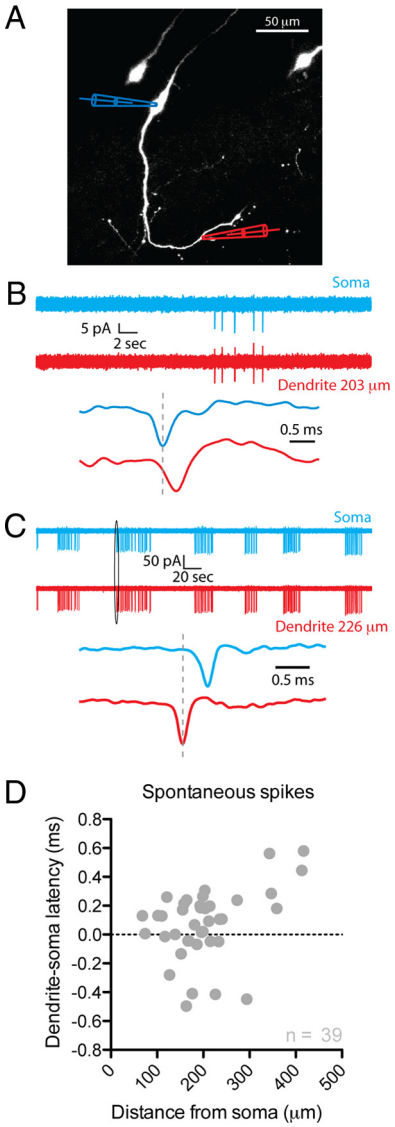

Figure 1. The dendrites of GnRH neurons propagate fast spikes. ***A***, Image of three GFP-GnRH neurons. Simultaneous loose-seal, on-cell recordings were performed from the soma and dendrite of the middle neuron as indicated. Blue, Somatic recording; red, dendritic recording. ***B***, The top panel shows a burst of five spikes recorded simultaneously at the somatic and dendritic on-cell recording sites from the neuron shown in ***A***. The bottom panel in ***B*** shows the first spike of the burst at a much higher time resolution. All spikes recorded in this neuron were seen at the somatic recording electrode before the dendritic recording electrode. ***C***, Dual on-cell recordings from a different GnRH neuron. This cell showed a spontaneous bursting pattern of action potential firing. In addition, all spikes were observed at the dendritic recording electrode before the somatic electrode. ***D***, The latency between spikes recorded at the somatic and dendritic locations is plotted against the site of the dendritic recording electrode for all spontaneously active neurons ($n = 39$ cells). Negative latencies indicate that spikes were recorded at the dendritic electrode before the somatic electrode.

the somatic eAP were given negative latencies and this dendrite was termed the initiating dendrite (i-dendrite). Dendritic eAPs that occurred after the somatic eAP were assigned positive latencies and the dendrite these were recorded in was termed the secondary dendrite (s-dendrite).

In five of eight cells, the GnRH neuron was bipolar and extracellular recordings were performed from both dendrites as well as the soma. In the three remaining cells, the GnRH neuron was unipolar. The latency between the extracellular spike recorded at the soma and at different dendritic locations was subsequently measured (see Materials and Methods). In seven of eight neurons, we found that the extracellular spike recorded in the i-dendrite occurred before the extracellular spike in the soma (Fig. 2). Importantly, of these cells, the spike latencies in the bipolar cells showed that the action potential was observed first in the i-dendrite, traveled through the soma, and then into s-dendrite. The mean distance from the soma at which the largest negative latency was recorded was 64 ± 17 μm ($n = 7$). The mean latency difference at this site was -0.25 ± 0.11 ms ($n = 7$). These data are consistent with the majority of GnRH neurons having the site of spike initiation in their dendrite.

Active and passive spike propagation in GnRH neuron dendrites

To investigate the role of passive versus active spike propagation, we performed dual recordings from the soma (whole cell) and dendrite (on cell). Dendritic on-cell recordings allowed us to record at much greater dendritic distances than with extracellular field potential recordings. The mean distance from the soma of dendritic recordings was 227.9 ± 36.5 μm ($n = 8$).

For these experiments, the soma was held in voltage clamp and an action potential voltage waveform was injected. This in turn evoked a spike at the dendritic recording electrode (Fig. 3*A*). To calculate the latency between the somatic and dendritic spike, we took the first derivative of the voltage command waveform (dV/dt) injected into the soma and then measured the latency between the peak dV/dt to the peak of the dendritic spike. It has been previously shown that the peak somatic dV/dt coincides with the peak of the on-cell recorded spike at the soma (Meeks et al., 2005; Atherton et al., 2008). In these experiments, three of eight cells showed spikes at the dendritic recording pipette before the peak dV/dt at the soma. We then bath-applied TTX (1 μM) and repeated the voltage-clamp protocol. TTX produced a large reduction in dendritic spike amplitude ($p < 0.05$; $n = 8$) (Fig. 3*B–D*) with spikes recorded at distal sites being inhibited to a greater extent ($r^2 = 0.70$; $p < 0.05$) (Fig. 3*D*). Importantly, all of the dendrite first spikes ($n = 3$ cells) shifted to soma first after application of TTX as would be predicted for passive electrotonic current spread into the dendrite after somatic current injection (Fig. 3*E*). These data further support the idea that GnRH neurons actively propagate Na^+ spikes along their dendrites.

The initial 150 μm of the dendrite have a high sodium channel density

It has previously been shown that GnRH neurons express Na^+ channels on their dendrites (Roberts et al., 2008); however, that immunohistochemistry was not sensitive enough to detect changes in channel density at different points along the dendrite. An alternative method to estimate the relative Na^+ channel density is to perform intracellular Na^+ imaging with Na^+-sensitive dyes (Meier et al., 2006; Kole et al., 2008; Fleidervish et al., 2010). We performed whole-cell recordings from GnRH neurons and loaded them with the Na^+-sensitive dye CoroNa Green (500 μM). We subsequently imaged the change in fluorescence in response to a burst of 10 action potentials at 10 Hz driven with depolarizing current through the somatic patch electrode. Four to six imaging sites were chosen from the soma or dendrite of each cell. Dendritic Na^+ transients could be abolished by bath applied TTX (1 μm) (data not shown).

We found that, in many cells, proximal regions of dendrite displayed large Na^+ transients in response to bursts of spikes. When we averaged the distance at which the largest Na^+ transient was observed in each cell during the burst, it was found to

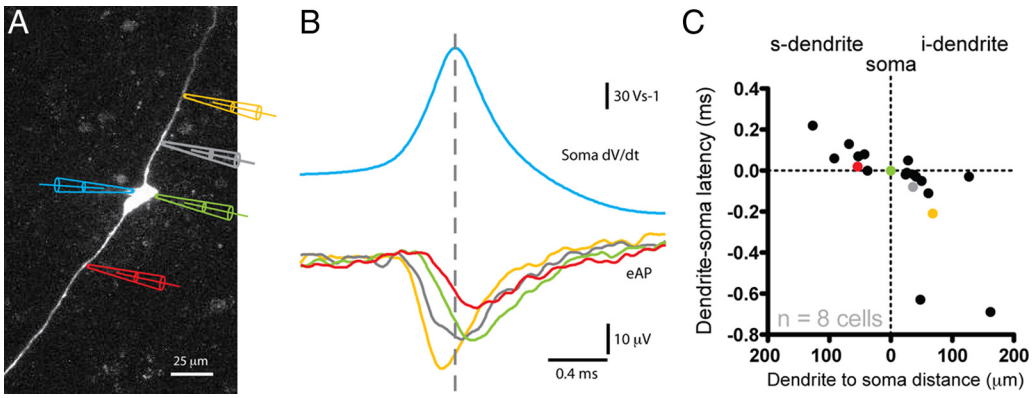

Figure 2. Multisite recordings from GnRH neuron dendrites confirms spikes in the dendrite before the soma. ***A***, Image of a GnRH neuron filled with Alexa Fluor 555 via the whole-cell recording electrode at the soma (left; blue pipette). An extracellular recording electrode was placed at different sites along the soma-dendritic axis (electrodes on the right of the cell colored yellow, gray, green, and red) to record the eAP. ***B***, Recordings from the neuron shown in ***A***. The color of the trace corresponds to the color of the electrode in ***A***. The top blue trace in ***B*** shows the first derivative of the whole-cell somatic action potential. The bottom traces are eAPs recorded at different locations along the soma-dendritic axis (yellow, 68 μm; gray, 36 μm; green, 0 μm; red, −54 μm). The peak of the eAP occurs first at the yellow recording electrode and last at the red. ***C***, Summary of 27 extracellular recording sites from 8 different GnRH neurons. Recordings from the neuron shown in ***A*** are color coded. Dendritic eAPs that occurred before the somatic eAP have negative latencies, whereas dendritic eAPs that occurred after the somatic eAP have positive latencies. We have defined the dendrite with negative spike latencies as the initiating dendrite (i-dendrite) and the dendrite with positive latencies as the secondary dendrite (s-dendrite).

occur at 65 ± 12 μm from the soma ($n = 8$). Interestingly, regions of dendrite from 0 to 150 μm from the soma all displayed large Na^+ transients while regions of dendrite >150 μm displayed either very small or no transients [average transient (ΔF) in the 0–150 μm of dendrite, 9.21 ± 2.23 AU, vs for 150–300 μm of dendrite, −1.06 ± 2.70 AU; $p = 0.007$; $n = 8$ cells, 34 imaging sites] (Fig. 4). If these data were reanalyzed using $\Delta F/F$, similar results were observed (Fig. 4*C*). There was no relationship between the size of the Na^+ transient and dendritic diameter (data not shown).

These data, together with the dendritic recording data, suggest that the proximal region of the GnRH neuron dendrite is highly excitable and support the hypothesis that GnRH neurons initiate action potentials in their dendrite.

Spike initiation site does not shift with somatic versus dendritic excitation

While all regions of the GnRH neuron dendrite appear to conduct Na^+ spikes, it is unclear whether the site of spike initiation can shift between different regions in response to somatic or distal dendritic excitation. To address this, we performed dual on-cell recordings from the soma and dendrite and puffed glutamate/glycine (1 mM) onto either the soma or dendrite (at the recording sites) and measured the latency between somatically and dendritically recorded spikes. The mean distance between the recording/puff sites was 257 ± 41 μm ($n = 6$). Changing the site of puff produced a small but nonsignificant shift in latency (soma puff mean latency, 0.22 ± 0.08 ms; dendrite puff mean latency, 0.18 ± 0.08 ms; $p > 0.05$; $n = 6$) (Fig. 5). In two of the six recordings, the neurons were spontaneously active before puffing began. In these two cells, the latency between the soma and dendritically recorded spontaneous spike was similar to that evoked by puffing (Fig. 5 includes representative traces showing this). Together, these data indicate that there is no shift in spike initiation site with somatic versus dendritic glutamate receptor stimulation. Therefore, the site of spike initiation appears to be relatively fixed.

Na^+ spikes evoke faithful Ca^{2+} transients in the dendrites of GnRH neurons

Several previous studies have investigated the effects of activity on Ca^{2+} signaling in the soma of adult GnRH neurons (Jasoni et al., 2007; Constantin et al., 2010; Lee et al., 2010). However, the effect of spiking in the dendrite has not been determined.

To investigate Ca^{2+} signaling in GnRH neuron dendrites, we loaded GnRH neurons with Rhod-2 Ca^{2+} indicator (200 μM) through the whole-cell patch pipette (Fig. 6*A*). Spikes were evoked by 5 ms somatic current injections. Both single spikes as well as bursts of three spikes (Fig. 6*B*,*C*) could evoke faithful Ca^{2+} transients in GnRH neuron dendrites for as far as the dendrite could be imaged in the slice (up to 458 μm; mean imaging distance, 190.7 ± 18.8 μm; $n = 27$). Interestingly, there was a significant correlation between the peak amplitude of the Ca^{2+} transient and the distance from the soma of the dendritic imaging site ($r^2 = 0.49$; $p < 0.05$) (Fig. 6*D*). The dendritic diameter was significantly smaller in more distal regions (diameter, 1.33 ± 0.08 μm at imaging sites <200 μm from soma, $n = 13$; diameter, 1.03 ± 0.06 μm at sites >200 μm from soma, $n = 14$; $p < 0.05$). There was also a significant correlation between the peak amplitude of the Ca^{2+} transient and the dendritic diameter ($r^2 = 0.41$; $p < 0.05$) with larger transients being seen in the smallest diameter dendrites. This suggests that the size of the dendritic Ca^{2+} transient increases as the dendritic volume decreases.

Next, we assessed the importance of dendritic voltage-gated Na^+ channels in mediating dendritic Ca^{2+} transients (Fig. 6*E*). In control conditions, three spikes at 8 Hz produced a peak dendritic Ca^{2+} transient of 0.51 ± 0.11 $\Delta F/F$ ($n = 6$). Local puffing of the voltage-gated Na^+ channel antagonist tetrodotoxin (TTX) (1 μM) on the dendrite next to the imaging site produced a marked inhibition of the spike evoked Ca^{2+} transient (28.1 ± 4.9% of control peak $\Delta F/F$ during TTX puff; $p < 0.05$; $n = 6$). This suggests that dendritic Na^+ spikes are responsible for the dendritic Ca^{2+} transients.

Next, we determined what pathways were responsible for the dendritic Ca^{2+} rises in response to a dendritic Na^+ spike. As before, we imaged dendritic Ca^{2+} in response to a burst of three spikes at 8 Hz in current clamp and then subsequently applied Ca^{2+} channel or sarcoplasmic/endoplasmic reticulum calcium ATPase (SERCA) pump antagonists (Fig. 6*F*). Bath application of these antagonists all caused increases in basal dendritic fluorescence levels, without any deterioration in apparent cell health. This change in baseline Ca^{2+} will lead to overestimates in the magnitude of the inhibition of Ca^{2+} transients when using $\Delta F/F$.

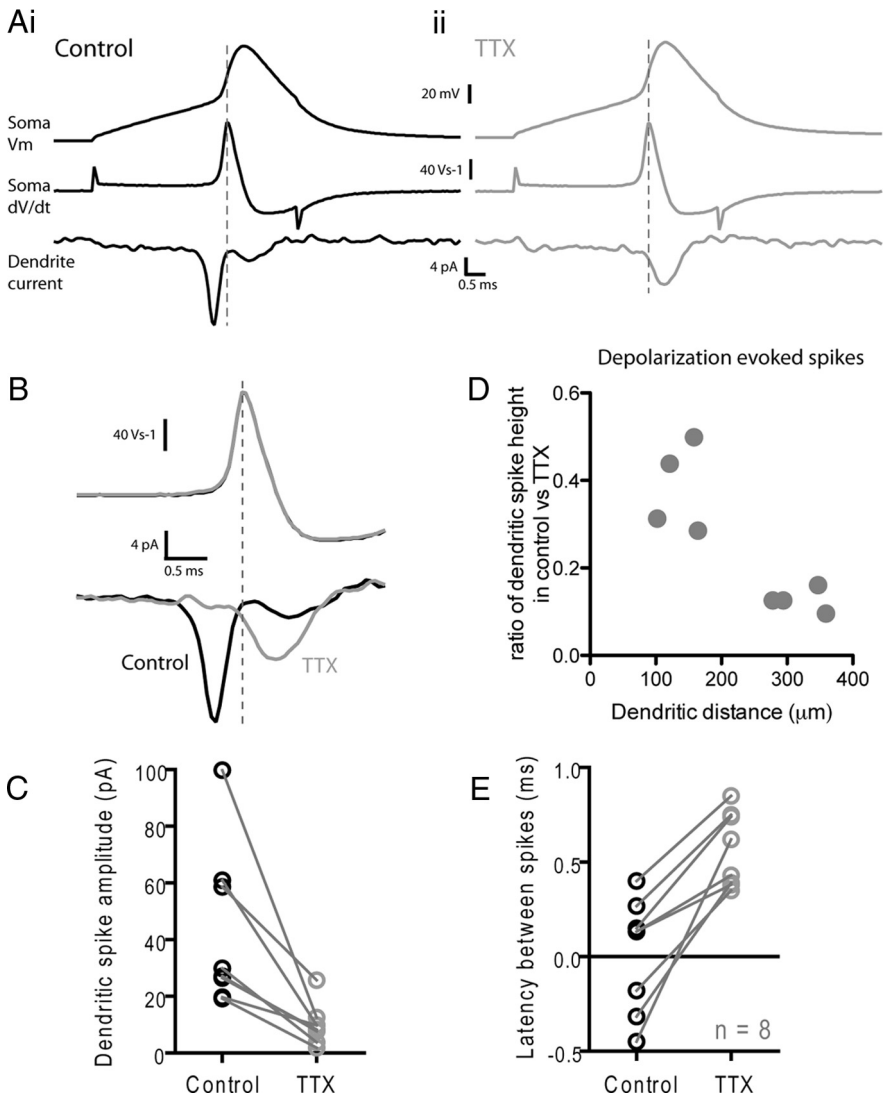

Figure 3. Properties of active and passive spike propagation in GnRH neuron dendrites. Whole-cell recordings were performed at the soma while simultaneous on-cell recordings were performed on the dendrite of GnRH neurons. ***Ai***, The soma was held in voltage clamp and an action potential waveform was injected into the cell (top trace). This induced a dendritic spike that was recorded in the on-cell recording electrode (bottom trace). The first derivative of the somatic membrane potential is shown in the middle trace. In the cell shown in ***Ai***, the peak of the dendritic spike comes before the peak of the first derivative of the somatic voltage. ***Aii***, After bath application of 1 μM TTX, the amplitude of the dendritic spike is reduced without affecting the amplitude of the voltage-clamp spike. ***B***, The effect of TTX on the dendritic spike recorded from the neuron in ***A*** is shown at a higher temporal resolution in ***B***. Black, Control; gray, after TTX. ***C***, Summary graph showing the effect of TTX on dendritic spike amplitude. ***D***, Summary graph showing that the effect of TTX on dendritic spike amplitude is greater for spikes recorded at greater distances from the soma. ***E***, Summary graph showing the effect of the latency of the dendritic spike before and after TTX. Negative latencies indicate that the peak of the dendritic spike occurred before the peak of the first derivative of the somatic voltage.

To overcome this problem, we did not normalize to the baseline and instead analyzed ΔF for these experiments.

The nonspecific Ca^{2+} channel antagonist $CdCl_2$ (200 μM) produced a large inhibition of the dendritic Ca^{2+} transient (peak ΔF Ca^{2+} transient, 24.1 ± 3.8% of control after 5 min $CdCl_2$; $p < 0.05$; $n = 4$). The L-type Ca^{2+} channel antagonist Nifedipine (50–100 μM) was also effective at inhibiting the peak Ca^{2+} transient (peak ΔF transient, 49.5 ± 7.2% of control after 15 min Nifedipine; $p < 0.05$; $n = 5$). Last, the T- and R-type Ca^{2+} channel antagonist $NiCl_2$ (200 μM) (Lee et al., 1999; Catterall et al., 2005) inhibited the peak Ca^{2+} transient to 66.1 ± 4.5% of control after 10 min ($n = 5$; $p < 0.05$) (Fig. 6*F*).

To test the involvement of Ca^{2+} release from internal stores, we inhibited store uptake with the SERCA pump inhibitor cyclopiazonic acid (CPA) (30 μM). CPA produced a small but significant inhibition of the dendritic Ca^{2+} transient (peak ΔF Ca^{2+} transient, 83.9 ± 5.1% of control after 10 min CPA; $p < 0.05$; $n = 5$). Bath application of 30 μM CPA could, however, markedly inhibit the rise in dendritic Ca^{2+} in response to bath-applied caffeine (30 mM) (data not shown), illustrating that, at this dose, CPA is effective at depleting Ca^{2+} stores.

Together, these data suggest that Na^+ spikes in GnRH neuron dendrites evoke Ca^{2+} rises through the opening of voltage-gated Ca^{2+} channels. There also appears to be dendritic Ca^{2+} release from internal stores during short bursts of spikes, similar to that which has been previously reported to occur in the soma of these neurons (Lee et al., 2010).

Discussion

Here, we provide insight into the functional properties of GnRH neuron dendrites. We show that action potentials are observed in one dendrite before the soma in the vast majority of GnRH neurons. These dendritic spikes propagate through the dendritic arbor for as far as we can record. The highest density of functional Na^+ channels is in the first 150 μm of dendrite and we suggest that this likely correlates with the site of spike initiation. Finally, dendritic Na^+ spikes in turn open dendritic voltage-gated Ca^{2+} channels, subsequently inducing dendritic Ca^{2+} transients. Together, these data support the idea that GnRH neurons can initiate action potentials in their proximal dendrite.

Previous studies have demonstrated that action potentials are seen first in the dendrite before the soma of some midbrain dopamine neurons and hippocampal interneurons (Häusser et al., 1995; Martina et al., 2000). However, the axon in many of these cells originates from the dendrite and not the soma. Thus, the axon is still the site of action potential initiation in these neurons (Häusser et al., 1995; Martina et al., 2000). Remarkably, the location of the GnRH neuron axon is presently unclear. As the processes that emanate from GnRH neuron soma often become thin in diameter, some laboratories have defined the thinnest process as the axon (Ybarra et al., 2011). However, previous work from our laboratory has demonstrated that, when cells are filled with biocytin in brain slices and *post hoc* reconstructed, processes containing dendritic spines and a dendritic morphology can easily be identified, but not axon-like processes (Campbell et al., 2005, 2009; Cottrell et al., 2006; Herde et al., 2011). Where then is the GnRH neuron axon? It has been shown that the terminal projection zone of GnRH neurons (the median eminence) contain GnRH fibers with secretary endings (Gross, 1976; Lehman et al., 1988; Yin et al., 2009). It is also known that GnRH neurons

extend very long dendrites, even up to 2 mm in length (Campbell et al., 2005) (Herde MK, Herbison AE, unpublished observations). Therefore, it seems likely that an axon forms somewhere along this very long trajectory. The question of where the axon originates in GnRH neurons will only be answered when a GnRH soma, dendrite, and axon is reconstructed in its full length. This is currently not possible in a conventional brain slice preparation and will likely require dye filling of neurons *in vivo*. It is important to note that we have only studied one region of the GnRH neuron dendrite (<500 μm from the soma). The properties of the distal regions of these dendrites await further study.

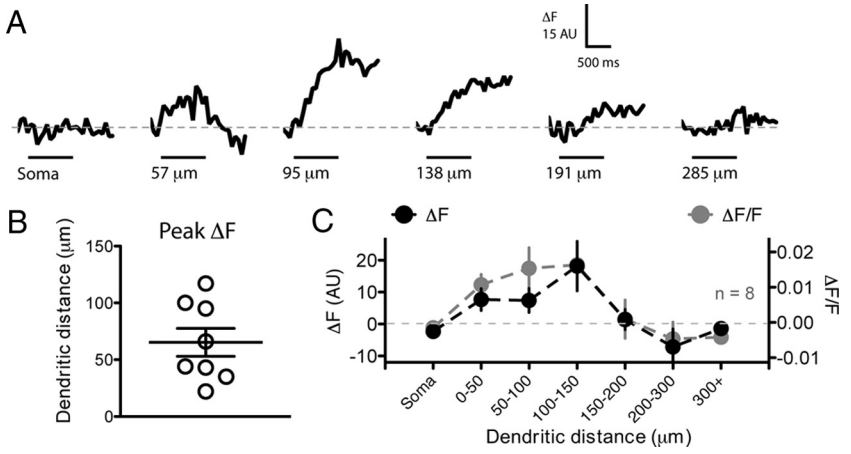

Figure 4. The initial 150 μm of the dendrite has a high sodium channel density. GnRH neurons were whole-cell loaded with 500 μM of the Na^+-sensitive dye CoroNa Green. After 15–20 min loading, neurons were induced to spike 10 times at 10 Hz with step depolarizations. Changes in CoroNa fluorescence were subsequently measured with frame scans on the soma and different regions of the dendrite. ***A*** shows Δ*F* traces from one neuron at six different imaging locations. The black bar under traces indicates the period of spiking at the soma. Each trace is the average of 5–10 trials. In this neuron, the largest Na^+ transient was observed at a site 95 μm from the soma. ***B***, The site of the largest Δ*F* Na^+ transient is plotted for eight different neurons. ***C***, The average Δ*F* (black) and Δ*F*/*F* (gray) per section of dendrite for eight neurons shows large Na^+ transients in the first 150 μm of dendrite but little or no transients at distances >150 μm. For the graph in ***C***, only the largest response per region of dendrite is plotted for each neuron.

If the proximal dendrite of GnRH neurons does not possess an axon, what implications does this have for spike initiation? The soma of a neuron has a much larger capacitance when compared with a small region of dendrite. Therefore, if the soma and dendrite had similar densities of voltage-gated conductances, the threshold for spike initiation would be lower in the dendrite than the soma. These considerations together with our dual electrical recording data, Na^+ imaging, and previous studies demonstrating the lack of a proximal axon, all point to the dendrite as the site of spike initiation in GnRH neurons. With single site on-cell dendritic recordings, we observed the action potential first in the dendrite before the soma in 30% of cells. We speculated that this low percentage was due to the fact that we were only sampling one dendritic location per neuron. Indeed, if we performed multisite recordings on both dendrites of bipolar cells, we observed spikes in one dendrite before the soma in seven of eight cells. In the one remaining cell, we were only able to record from one site on each dendrite as well as the soma before the recording deteriorated. It is highly likely that the spike initiation site is also in the dendrite of this one neuron, however, at a site closer to the soma than to the dendritic recording sites.

While we were able to perform multiple extracellular recordings of dendritic spikes from the proximal dendrite, we were unable to record extracellular spikes consistently at more distal dendritic sites. This is likely due to the fact that the extracellular field spike is mediated predominantly by ionic conductances, mostly Na^+ (Palmer et al., 2010). As we found the density of functional Na^+ channels decreases at distances >150 μm away from the soma, this may explain our lack of ability to record spike-evoked field potentials at these distal sites.

Capacitive currents primarily mediate spikes recorded in the on-cell configuration. With this technique, we were able to perform dendritic recordings up to 417 μm away from the soma. In five neurons, we obtained recordings between 300 and 417 μm along a dendrite and interestingly, none of these five cells exhibited spikes first in the dendritic electrode before the somatic. This, together with our other data, suggests that the site of action potential initiation may be in the proximal dendrite, likely within the first 200 μm. If the site of initiation were in the distal dendrite (>300 μm away from the soma), then one would expect a higher percentage of spikes being seen first in the dendritic recording electrode in this set of experiments.

Our Na^+ imaging experiments revealed that the first 150 μm of dendrite exhibited the largest increase in CoroNa fluorescence in response to a 1 s burst of 10 action potentials. This suggests that the largest Na^+ flux occurs in this region of dendrite. Very small or no Na^+ transients were observed in the soma of GnRH neurons. This may be due to two things: First, the large volume of the soma would act to effectively dilute Na^+. Thus, for the same Na^+ influx, there would be a smaller change in Na^+ concentration in the soma compared with a low volume dendrite. Second, the affinity of the CoroNa Green Na^+ indicator for Na^+ is low (K_d, ~80 mM), thus making it difficult to detect very small change in intracellular Na^+.

The first study to suggest the dendrite as the site of action potential initiation in GnRH neurons also showed through immunohistochemistry that the dendrites of these neurons express voltage-gated Na^+ channels (Roberts et al., 2008). That study also generated a morphologically based computer model of a GnRH neuron soma and dendrite. In this neuron model, the threshold for dendritic spike initiation decreases at increasing distances along the dendrite rather than being lowest in the proximal dendrite. One possible explanation for the discrepancy between the model and our data is that there is a higher density of voltage-gated Na^+ channels in the proximal dendrite of GnRH neurons than used in the model, thus making the proximal dendrite much more excitable. The effect of varying proximal Na^+ channel densities on dendritic spike initiation would be interesting to investigate in future models.

Dendritic spikes in most neurons are associated with dendritic Ca^{2+} rises. We have demonstrated that this is also the case in the dendrites of GnRH neurons, even at distances >300 μm from the soma. Ca^{2+} signaling in the soma of GnRH neurons has been proposed to regulate burst firing through the opening of Ca^{2+}-activated K^+ channels (Lee et al., 2010). This may also occur in the dendrite; however, dendritic Ca^{2+} rises could also drive the release of dendritic messengers (Chu and Moenter, 2005). As the dendrites of GnRH neurons bundle with one another (Campbell et al., 2009), dendritic transmitter release may facilitate synchro-

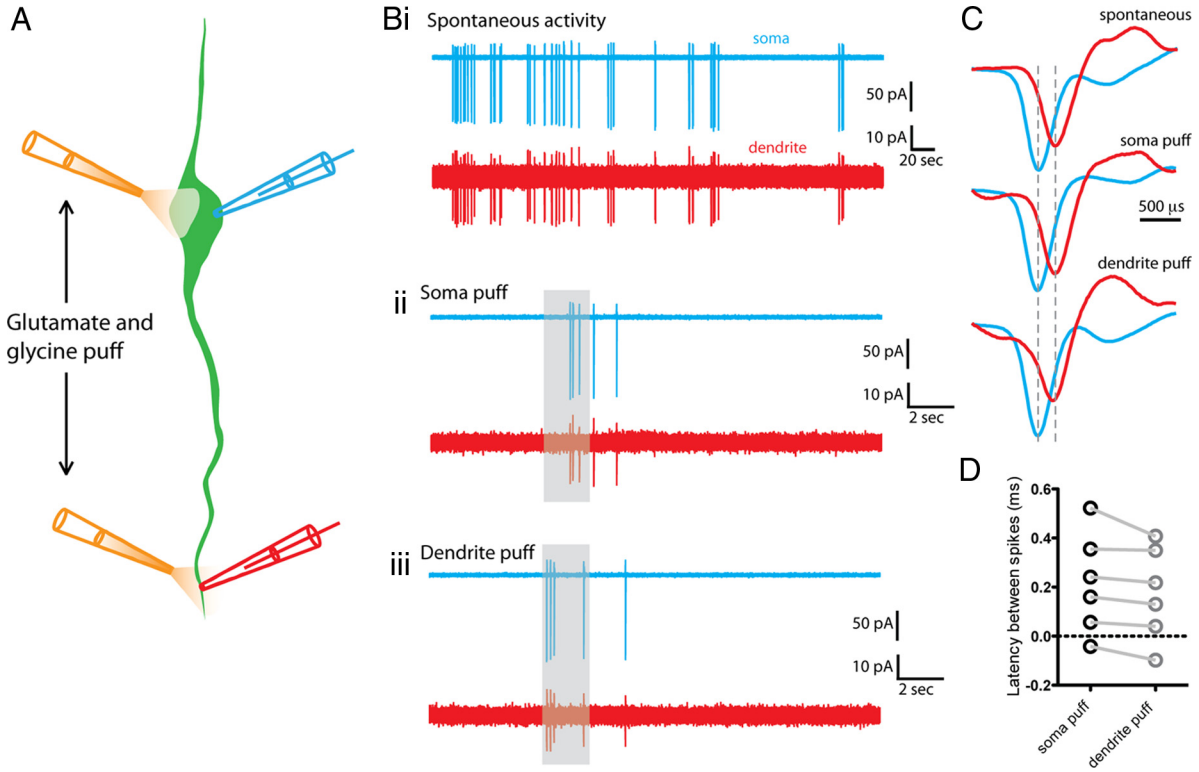

Figure 5. Spike initiation site does not shift with proximal versus distal dendritic excitation. ***A***, Diagram illustrating the experimental configuration. Dual on-cell recordings were performed from the soma and dendrite of a GnRH neuron. A puff electrode was positioned close to either the soma or dendrite recording site. Spikes were evoked by a 2 s puff of glutamate and glycine (1 mM) at each site. ***B***, Traces showing the spiking activity recorded at both the soma (blue) and dendrite (red) of a single neuron either spontaneously (***Bi***) or evoked by somatic (***Bii***) or dendritic (***Biii***) glutamate/glycine puff. The duration of the puff is indicated by the gray bar. ***C***, The timing of individual spikes is shown for both spontaneous and puff evoked spiking. In this cell, the somatic spike preceded the dendritic spike in all conditions. Blue spikes, Somatically recorded; red spikes, dendritically recorded. ***D***, Summary graph showing that the latency between somatically and dendritically recorded spikes does not change with somatic versus dendritic glutamate/glycine puff.

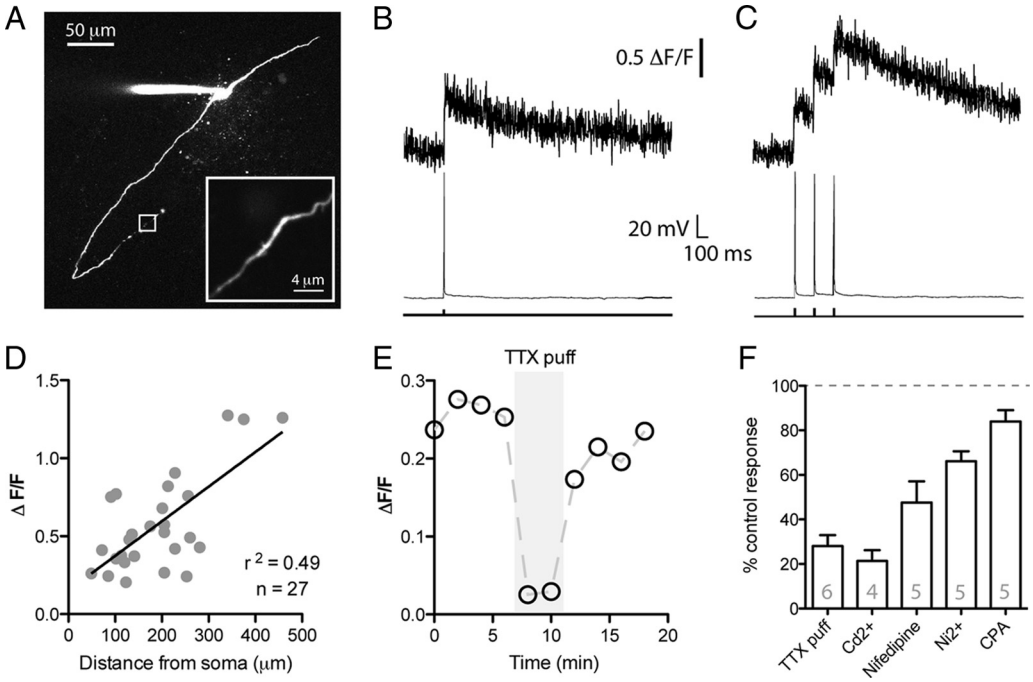

Figure 6. Na^{+} spikes evoke Ca^{2+} rises in GnRH neuron dendrites. ***A***, Confocal stack of a Rhod-2 loaded GnRH neuron. The inset shows a region of dendrite 458 μm from the soma that was line scan imaged. ***B***, ***C***, Ca^{2+} transients recorded from the neuron shown in ***A*** in response to either a single spike or three spikes evoked by depolarizing current injection at the soma. ***D***, There is a trend for larger peak Ca^{2+} transients in more distal regions of GnRH neuron dendrites. Each data point is taken from a different cell ($n = 27$). ***E***, Local puff application of TTX to the dendrite produces a robust inhibition in the spiking-induced Ca^{2+} transient. Response shown is from a single cell. ***F***, Summary data showing the percentage of the spike-evoked dendritic Ca^{2+} transient that remained after various pharmacological manipulations. All treatments resulted in a significant ($p < 0.05$) reduction in peak transient amplitude. Error bars indicate SEM.

nization between GnRH neurons similar to that proposed for magnocellular oxytocin neurons (Lambert et al., 1993). Dendritic Ca^{2+} rises will also be important in determining the direction and magnitude of synaptic plasticity in GnRH neurons. Whether synapses onto GnRH neuron dendrites display classical long-term plasticity or spike timing-dependent plasticity has yet to be investigated in this neuronal population.

In summary, using multiple approaches we suggest that action potentials are initiated within the proximal region of one GnRH neuron dendrite. These Na^+ spikes propagate throughout the dendrite and subsequently induce dendritic Ca^{2+} rises. As the highest density of putative excitatory synaptic inputs onto GnRH neurons also occur in the proximal dendrite (Campbell et al., 2005), a proximal dendritic site of action potential initiation likely represents an efficient location to integrate subthreshold inputs into spiking output.

References

Atherton JF, Wokosin DL, Ramanathan S, Bevan MD (2008) Autonomous initiation and propagation of action potentials in neurons of the subthalamic nucleus. J Physiol 586:5679–5700.

Campbell RE, Han SK, Herbison AE (2005) Biocytin filling of adult gonadotropin-releasing hormone neurons in situ reveals extensive, spiny, dendritic processes. Endocrinology 146:1163–1169.

Campbell RE, Gaidamaka G, Han SK, Herbison AE (2009) Dendrodendritic bundling and shared synapses between gonadotropin-releasing hormone neurons. Proc Natl Acad Sci U S A 106:10835–10840.

Catterall WA, Perez-Reyes E, Snutch TP, Striessnig J (2005) International Union of Pharmacology. XLVIII. Nomenclature and structure-function relationships of voltage-gated calcium channels. Pharmacol Rev 57:411–425.

Chen WR, Midtgaard J, Shepherd GM (1997) Forward and backward propagation of dendritic impulses and their synaptic control in mitral cells. Science 278:463–467.

Chu Z, Moenter SM (2005) Endogenous activation of metabotropic glutamate receptors modulates GABAergic transmission to gonadotropin-releasing hormone neurons and alters their firing rate: a possible local feedback circuit. J Neurosci 25:5740–5749.

Colbert CM, Pan E (2002) Ion channel properties underlying axonal action potential initiation in pyramidal neurons. Nat Neurosci 5:533–538.

Constantin S, Jasoni CL, Wadas B, Herbison AE (2010) Gamma-aminobutyric acid and glutamate differentially regulate intracellular calcium concentrations in mouse gonadotropin-releasing hormone neurons. Endocrinology 151:262–270.

Cottrell EC, Campbell RE, Han SK, Herbison AE (2006) Postnatal remodeling of dendritic structure and spine density in gonadotropin-releasing hormone neurons. Endocrinology 147:3652–3661.

Fleidervish IA, Lasser-Ross N, Gutnick MJ, Ross WN (2010) Na^+ imaging reveals little difference in action potential-evoked Na^+ influx between axon and soma. Nat Neurosci 13:852–860.

Golding NL, Spruston N (1998) Dendritic sodium spikes are variable triggers of axonal action potentials in hippocampal CA1 pyramidal neurons. Neuron 21:1189–1200.

Gross DS (1976) Distribution of gonadotropin-releasing hormone in the mouse brain as revealed by immunohistochemistry. Endocrinology 98:1408–1417.

Häusser M, Stuart G, Racca C, Sakmann B (1995) Axonal initiation and active dendritic propagation of action potentials in substantia nigra neurons. Neuron 15:637–647.

Herbison AE, ed (2006) Physiology of the GnRH neuronal network, Ed 3. San Diego: Academic.

Herde MK, Geist K, Campbell RE, Herbison AE (2011) Gonadotropin-releasing hormone neurons extend complex highly branched dendritic trees outside the blood-brain barrier. Endocrinology 152:3832–3841.

Hu W, Tian C, Li T, Yang M, Hou H, Shu Y (2009) Distinct contributions of $Na_v1.6$ and $Na_v1.2$ in action potential initiation and backpropagation. Nat Neurosci 12:996–1002.

Jasoni CL, Todman MG, Strumia MM, Herbison AE (2007) Cell type-specific expression of a genetically encoded calcium indicator reveals intrinsic calcium oscillations in adult gonadotropin-releasing hormone neurons. J Neurosci 27:860–867.

Jennes L, Stumpf WE, Sheedy ME (1985) Ultrastructural characterization of gonadotropin-releasing hormone (GnRH)-producing neurons. J Comp Neurol 232:534–547.

Kole MH, Ilschner SU, Kampa BM, Williams SR, Ruben PC, Stuart GJ (2008) Action potential generation requires a high sodium channel density in the axon initial segment. Nat Neurosci 11:178–186.

Lambert RC, Moos FC, Richard P (1993) Action of endogenous oxytocin within the paraventricular or supraoptic nuclei: a powerful link in the regulation of the bursting pattern of oxytocin neurons during the milk-ejection reflex in rats. Neuroscience 57:1027–1038.

Lee JH, Gomora JC, Cribbs LL, Perez-Reyes E (1999) Nickel block of three cloned T-type calcium channels: low concentrations selectively block alpha1H. Biophys J 77:3034–3042.

Lee K, Duan W, Sneyd J, Herbison AE (2010) Two slow calcium-activated afterhyperpolarization currents control burst firing dynamics in gonadotropin-releasing hormone neurons. J Neurosci 30:6214–6224.

Lehman MN, Karsch FJ, Robinson JE, Silverman AJ (1988) Ultrastructure and synaptic organization of luteinizing hormone-releasing hormone (LHRH) neurons in the anestrous ewe. J Comp Neurol 273:447–458.

Martina M, Vida I, Jonas P (2000) Distal initiation and active propagation of action potentials in interneuron dendrites. Science 287:295–300.

Meeks JP, Jiang X, Mennerick S (2005) Action potential fidelity during normal and epileptiform activity in paired soma-axon recordings from rat hippocampus. J Physiol 566:425–441.

Meier SD, Kovalchuk Y, Rose CR (2006) Properties of the new fluorescent Na^+ indicator CoroNa Green: comparison with SBFI and confocal Na^+ imaging. J Neurosci Methods 155:251–259.

Moenter SM, DeFazio AR, Pitts GR, Nunemaker CS (2003) Mechanisms underlying episodic gonadotropin-releasing hormone secretion. Front Neuroendocrinol 24:79–93.

Palmer LM, Clark BA, Gründemann J, Roth A, Stuart GJ, Häusser M (2010) Initiation of simple and complex spikes in cerebellar Purkinje cells. J Physiol 588:1709–1717.

Roberts CB, Campbell RE, Herbison AE, Suter KJ (2008) Dendritic action potential initiation in hypothalamic gonadotropin-releasing hormone neurons. Endocrinology 149:3355–3360.

Spergel DJ, Krüth U, Hanley DF, Sprengel R, Seeburg PH (1999) GABA- and glutamate-activated channels in green fluorescent protein-tagged gonadotropin-releasing hormone neurons in transgenic mice. J Neurosci 19:2037–2050.

Stuart GJ, Sakmann B (1994) Active propagation of somatic action potentials into neocortical pyramidal cell dendrites. Nature 367:69–72.

Wray S, Hoffman G (1986) Postnatal morphological changes in rat LHRH neurons correlated with sexual maturation. Neuroendocrinology 43:93–97.

Ybarra N, Hemond PJ, O'Boyle MP, Suter KJ (2011) Spatially selective, testosterone-independent remodeling of dendrites in gonadotropin-releasing hormone (GnRH) neurons prepubertally in male rats. Endocrinology 152:2011–2019.

Yin W, Mendenhall JM, Monita M, Gore AC (2009) Three-dimensional properties of GnRH neuroterminals in the median eminence of young and old rats. J Comp Neurol 517:284–295.